

# Molecular H<sub>2</sub>O as carrier for oxygen diffusion in hydrous silicate melts

H. Behrens<sup>a,\*</sup>, Y. Zhang<sup>b</sup>, M. Leschik<sup>a,c</sup>, M. Wiedenbeck<sup>d</sup>,  
G. Heide<sup>c</sup>, G.H. Frischat<sup>c</sup>

<sup>a</sup> *Institut für Mineralogie, Universität Hannover, Callinstr. 3, D-30167 Hannover, Germany*

<sup>b</sup> *Department of Geological Sciences, The University of Michigan, Ann Arbor, MI 48109-1063, USA*

<sup>c</sup> *Institut für Nichtmetallische Werkstoffe, TU Clausthal, Zehntnerstr. 2a, D-38678 Clausthal-Zellerfeld, Germany*

<sup>d</sup> *GeoForschungsZentrum Potsdam, Telegrafenberg, D-14473 Potsdam, Germany*

Received 3 September 2005; received in revised form 12 November 2006; accepted 13 November 2006

Available online 22 December 2006

Editor: R.D. van der Hilst

## Abstract

Dissolved water is known to dramatically enhance oxygen diffusion in silicate melts, glasses and minerals. A quantitative theory has been developed to explain this phenomenon by transport via molecular H<sub>2</sub>O diffusion [Y. Zhang, E.M. Stolper, G.J. Wasserburg, Diffusion of a multi-species component and its role in the diffusion of water and oxygen in silicates, *Earth Planet. Sci. Lett.*, 103 (1991) 228–240.]. Here we report experimental confirmation of the theory for rhyolitic melts by measuring both H<sub>2</sub>O and <sup>18</sup>O diffusion profiles in a single experiment. In sorption experiments at 100 MPa and temperatures from 1041 to 1136 K isotopically enriched water diffused into doubly polished rhyolitic glass wafers. H<sub>2</sub>O profiles were analyzed by infrared spectroscopy and <sup>18</sup>O profiles by SIMS. <sup>18</sup>O diffusivities were found to be 1–2 orders of magnitude slower than bulk water diffusivities but 3–4 orders of magnitude faster than Eyring diffusivities calculated from viscosity. The data show that oxygen “self” diffusion under hydrothermal conditions is due to molecular H<sub>2</sub>O diffusion, not due to the self diffusion of oxygen itself. With this confirmation, experimental data on H<sub>2</sub>O diffusion in silicate melts can be used to infer <sup>18</sup>O diffusion under hydrothermal conditions, and hydrothermal oxygen diffusion data in silicate minerals can be used to infer H<sub>2</sub>O diffusivity, as long as the concentration or solubility of H<sub>2</sub>O in the given phase is known.

© 2006 Elsevier B.V. All rights reserved.

**Keywords:** oxygen diffusion; hydrous silicate melts; rhyolite; H<sub>2</sub>O diffusion; oxygen and hydrogen isotopes

## 1. Introduction

Many authors have carried out <sup>18</sup>O “self” diffusion experiments under hydrothermal conditions [2–9]. During such an experiment, an <sup>18</sup>O-enriched H<sub>2</sub>O

fluid surrounds or is in contact with a mineral, glass or melt, and <sup>18</sup>O diffuses into the condensed phase. After the experiment, the isotopic ratio  $R$  ( $\equiv$  <sup>18</sup>O/(<sup>16</sup>O + <sup>18</sup>O)) is measured as a function of distance from the surface in contact with the fluid. Experimental data show that the presence of water dramatically enhances <sup>18</sup>O diffusivity. Related phenomena are the hydrolytic weakening of quartz [10,11] and enhanced cation diffusivities in framework silicates such as feldspars [12–14].

\* Corresponding author. Tel.: +49 511 762 8054; fax: +49 511 762 3504.

E-mail address: [h.behrens@mineralogie.uni-hannover.de](mailto:h.behrens@mineralogie.uni-hannover.de)  
(H. Behrens).

Various hypotheses have been proposed to explain the dramatic enhancement of oxygen diffusion in silicate melts [1,15–24]. The most often discussed explanations are based on the enhancements induced by fast proton transients [18–20] or hydrous species as carriers of oxygen [21–24]. The former is a qualitative idea and has not been developed into a quantitative theory. The latter hypothesis suggests that hydrothermal oxygen “self” diffusion data actually reflect transport via H<sub>2</sub>O diffusion for which a quantitative theory has been proposed.

It is well established that molecular H<sub>2</sub>O (hereafter referred to as H<sub>2</sub>O<sub>m</sub>) is the mobile species responsible for transporting the H<sub>2</sub>O component in silicate melts [25–31] although some details about migration of H<sub>2</sub>O in the melts remain debated [25,32,33]. OH is essentially immobile but may be consumed or regenerated by an interconversion reaction between H<sub>2</sub>O and OH. Hence, diffusion of H<sub>2</sub>O is a classical diffusion-reaction problem [34]. The diffusion coefficient of total H<sub>2</sub>O (H<sub>2</sub>O<sub>t</sub>, including both H<sub>2</sub>O<sub>m</sub> and hydroxyl) can be expressed as:

$$D_{\text{H}_2\text{O}_t} = D_{\text{H}_2\text{O}_m} \cdot dX_{\text{H}_2\text{O}_m}/dX_{\text{H}_2\text{O}_t}. \quad (1)$$

Where  $X$  refers to the mole fraction of the species or component in the melt calculated on a single oxygen basis. Because H<sub>2</sub>O contains oxygen, the diffusion of H<sub>2</sub>O<sub>m</sub> leads to an oxygen flux. A number of authors [1,7,9,18,22–24] have proposed that <sup>18</sup>O diffusion from a hydrothermal fluid into silicate melt, glass, quartz and feldspar is carried by H<sub>2</sub>O<sub>m</sub>, with anhydrous oxygen and OH being essentially immobile except for local <sup>18</sup>O–<sup>16</sup>O isotopic exchange reactions between H<sub>2</sub>O<sub>m</sub> and other oxygen species. That is, <sup>18</sup>O transport from a hydrothermal fluid into a silicate melt, glass or mineral is controlled by coupled diffusion and exchange. Detailed quantitative aspects of this mechanism have been developed by Zhang et al. [1] but experimental evidence has, until now, been missing. Although an accurate general expression for  $D_{^{18}\text{O}}$  (the apparent <sup>18</sup>O diffusivity) is complicated, an approximate expression is as follows [1]:

$$D_{^{18}\text{O}} \approx D_{\text{H}_2\text{O}_m} \cdot X_{\text{H}_2\text{O}_m}. \quad (2)$$

Combining Eqs. (1) and (2) leads to,

$$D_{^{18}\text{O}} \approx D_{\text{H}_2\text{O}_t} \cdot X_{\text{H}_2\text{O}_m} \cdot dX_{\text{H}_2\text{O}_t}/dX_{\text{H}_2\text{O}_m}. \quad (3)$$

At very low  $X_{\text{H}_2\text{O}_t}$  (<0.001) which are typically found in nominally water-free minerals, this equation simplifies to

$$D_{^{18}\text{O}} \approx D_{\text{H}_2\text{O}_t} \cdot X_{\text{H}_2\text{O}_t}/2. \quad (4)$$

Hence,  $D_{^{18}\text{O}}$  is typically orders of magnitude smaller than  $D_{\text{H}_2\text{O}_t}$  and the <sup>18</sup>O profile is much shorter than the H<sub>2</sub>O<sub>t</sub> profile. Therefore, across the <sup>18</sup>O profile, H<sub>2</sub>O<sub>t</sub> is roughly constant, leading to constant  $D_{^{18}\text{O}}$  and an error function shape of the profile [4–8]. On the other hand, when surface  $X_{\text{H}_2\text{O}_t}$  is large (as for hydrous melts in contact with a fluid),  $D_{^{18}\text{O}}$  approaches  $D_{\text{H}_2\text{O}_t}$  and the length of <sup>18</sup>O profile is a significant portion of that of the H<sub>2</sub>O<sub>m</sub> profile. That is, along the <sup>18</sup>O profile,  $X_{\text{H}_2\text{O}_t}$  and hence  $D_{^{18}\text{O}}$  vary significantly, leading to deviation of the shape of the <sup>18</sup>O profile from an error function. Numerical simulations show that when surface  $X_{\text{H}_2\text{O}_t}$  is <0.01, <sup>18</sup>O profile is essentially indistinguishable from an error function profile. When surface  $X_{\text{H}_2\text{O}_t}$  is >0.01, the deviation from an error function begins to be noticeable.

A definitive test for the above hypothesis involves the simultaneous measurement of profiles of both <sup>18</sup>O and hydrous species. If the hypothesis is correct, the two profiles would be related such that the <sup>18</sup>O profile can be calculated from the H<sub>2</sub>O<sub>t</sub> profile. In this study, we report such a confirmation by experiments in which <sup>18</sup>O-labeled (as well as D-labeled) water was diffused into polished rhyolitic glass wafers. Rhyolite was chosen because a large database for water diffusion is available for comparison. After the experiments, both profiles of H<sub>2</sub>O<sub>t</sub> and <sup>18</sup>O were measured: H<sub>2</sub>O<sub>t</sub> as the sum of OH and H<sub>2</sub>O<sub>m</sub> by infrared spectroscopy, and <sup>18</sup>O/<sup>16</sup>O by secondary ion mass spectrometry.  $R$  is calculated from <sup>18</sup>O/<sup>16</sup>O. We fit profiles of both H<sub>2</sub>O<sub>t</sub> and  $R$  assuming (i) H<sub>2</sub>O<sub>m</sub> is the diffusing species for both H<sub>2</sub>O<sub>t</sub> and <sup>18</sup>O, and (ii) diffusivity of H<sub>2</sub>O<sub>m</sub> is an exponential function of H<sub>2</sub>O<sub>t</sub> content [1]. Verification of the theory requires that both H<sub>2</sub>O<sub>t</sub> and  $R$  profiles would be well fit by a single expression of  $D_{\text{H}_2\text{O}_m}$ .

These experiments are relevant not only to understand oxygen diffusion in silicate melts, but also shed some light on the kinetics of hydrogen and oxygen isotope exchange between silicates and other phases. Practical applications of this work include estimation of oxygen diffusivity under hydrothermal conditions from water diffusivity, and vice versa.

## 2. Experiments and analyses

In the experiments doubly polished rhyolitic glass sections (1 × 5 × 5 mm) were sealed with isotopically enriched water in gold capsules. One natural obsidian containing 0.16 wt.% H<sub>2</sub>O<sub>t</sub> was run at 1085 K whereas in two other experiments a water-poor (0.04 wt.% H<sub>2</sub>O<sub>t</sub>) synthetic glass with a similar composition was used (Table 1). The starting fluid for the experiments at 1136 K and 1085 K contained D<sub>2</sub><sup>18</sup>O, with D/(D+H)=0.80 and R=0.855. In

Table 1  
Composition of glasses (wt.%)

Sample name sources	EDF Erevan Dry Fountain, Armenia	EDFS synthetic
SiO <sub>2</sub>	76.78 (0.32)	76.32 (0.28)
TiO <sub>2</sub>	0.10 (0.02)	0.01 (0.02)
Al <sub>2</sub> O <sub>3</sub>	12.77 (0.13)	13.27 (0.19)
FeO <sup>a)</sup>	0.52 (0.03)	0.01 (0.01)
MnO	0.09 (0.01)	0.00 (0.01)
MgO	0.07 (0.01)	0.01 (0.01)
CaO	0.56 (0.02)	1.11 (0.06)
Na <sub>2</sub> O	4.08 (0.07)	4.24 (0.11)
K <sub>2</sub> O	4.55 (0.07)	5.11 (0.11)
H <sub>2</sub> O <sup>b)</sup>	0.16	0.04
Sum	99.67	100.11
<i>M</i> <sub>glass</sub> (g/mol) <sup>c)</sup>	32.49	32.56

Notes. Each analysis is based on 10 measurements using a CAMECA SX100 electron microprobe (conditions: 15 kV acceleration voltage, 6–20 nA beam current, electron beam defocused to 20–40 μm diameter). 1σ uncertainties of microprobe data are given in parentheses.

<sup>a</sup> Total iron is given as FeO.

<sup>b</sup> The H<sub>2</sub>O content was determined from the peak height of the IR absorption band at 3570 cm<sup>-1</sup> using the calibration of Leschik et al. [35].

<sup>c</sup> Molar mass of anhydrous glass is calculated on single oxygen basis, and is needed for calculating the mole fractions of total H<sub>2</sub>O [40].

the experiment at 1041 K, the starting water was a 1:1 mixture of H<sub>2</sub><sup>18</sup>O with normal hydrogen and *R*=0.95 and D<sub>2</sub>O with normal oxygen and D/(D+H)=0.999, leading to *R* ≈ 0.48 and D/(D+H) ≈ 0.50.

Hydrothermal hydration experiments were carried out in rapid-quench externally heated pressure vessels at 100 MPa argon pressure. The capsule was stored in the water-cooled part of the vessel during heating. After reaching the target temperature the capsule was rapidly inserted into the hot part by rotating the vessel. To terminate the experiment, the sample was rapidly returned to the cold part. The experimental conditions are listed in Table 2. After cooling the samples were

sectioned perpendicular to the polished surface. H<sub>2</sub>O and D<sub>2</sub>O concentration profiles of the sections were determined by Fourier transform infrared spectroscopy (FTIR) at the University of Hannover. Concentrations were derived from the peak height of the band at 3570 cm<sup>-1</sup> (H<sub>2</sub>O) and 2650 cm<sup>-1</sup> (D<sub>2</sub>O) using calibrations of Leschik et al. [35]. Although different hydrogen isotopes were measured, we did not distinguish these isotopes in fitting the diffusion profiles but use the sum of both. <sup>18</sup>O/<sup>16</sup>O profiles were determined by secondary ion mass spectrometry (SIMS) at GeoForschungsZentrum Potsdam. Details of the analytical conditions are reported elsewhere [35]. When possible, multiple profiles were measured, and these profiles adjusted by shifting the surface position by no more than 3 μm parallel to the diffusion direction to make the multiple profiles consistent. In the experiment at 1041 K the amount of added fluid was probably too low to surround completely the sample and <sup>18</sup>O surface concentrations vary widely. Only the profile with the highest surface <sup>18</sup>O/<sup>16</sup>O ratio has been used in data treatment.

### 3. Experimental results

Profiles of H<sub>2</sub>O<sub>t</sub> and *R* are shown in Fig. 1. The surface H<sub>2</sub>O<sub>t</sub> content is roughly in agreement with H<sub>2</sub>O solubility data indicating about 4 wt.% H<sub>2</sub>O can be dissolved in rhyolitic melts at 100 MPa in the investigated temperature range [35–42]. H<sub>2</sub>O<sub>t</sub> profiles clearly do not follow an error function, indicating strong dependence of H<sub>2</sub>O diffusivity on H<sub>2</sub>O<sub>t</sub> content, as shown by numerous previous studies [25–32]. The <sup>18</sup>O profiles, although similar to an error function shape to the first order, also deviate slightly and resolvably from error function fits (dashed curves in Fig. 1), in particular at low *R* values. This is expected because the length of the *R* profile is significant compared to that of the H<sub>2</sub>O<sub>t</sub> profile. Typically, the *R*

Table 2  
Experimental conditions and fitting results

Exp #	<i>T</i> (K)	<i>P</i> (MPa)	Starting glass	<i>C</i> <sub>H<sub>2</sub>O<sub>t</sub></sub> initial (wt.%)	<i>R</i> fluid initial	D/(D+H) fluid initial	Time (s)	<i>X</i> <sub>H<sub>2</sub>O<sub>t</sub></sub> surface	<i>C</i> <sub>H<sub>2</sub>O<sub>t</sub></sub> surface (wt.%)	Best-fit <sup>a)</sup> <i>a</i>	<i>D</i> <sub>0</sub> based on H <sub>2</sub> O <sub>t</sub> fit	<i>D</i> <sub>0</sub> based on <sup>18</sup> O fit
1	1041	100	EDFS	0.04	≈ 0.48	≈ 0.50	2160	0.0756	4.33	34	1.89 ± 0.02	1.95 ± 0.05
2	1085	100	EDF	0.16	0.855	0.80	1830	0.0775	4.44	25	4.01 ± 0.07	4.98 ± 0.12
3	1136	100	EDFS	0.04	0.855	0.80	900	0.0750	4.29	18	10.5 ± 0.3	11.8 ± 0.2

Notes. 2σ uncertainties are shown for *D*<sup>0</sup> values obtained by fitting. Although fitting errors on *D*<sub>0</sub> are very small, the real error of diffusivities (including uncertainty on the position of the interface, spatial resolution, temperature, etc.) is likely on the order of 30%.

<sup>a</sup> The best-fit *a* values are somewhat different from those in Zhang and Behrens [28] because *a* values given there are not well constrained. Data in this study can be used to further constrain the dependence of *a* on *T* and *P*.

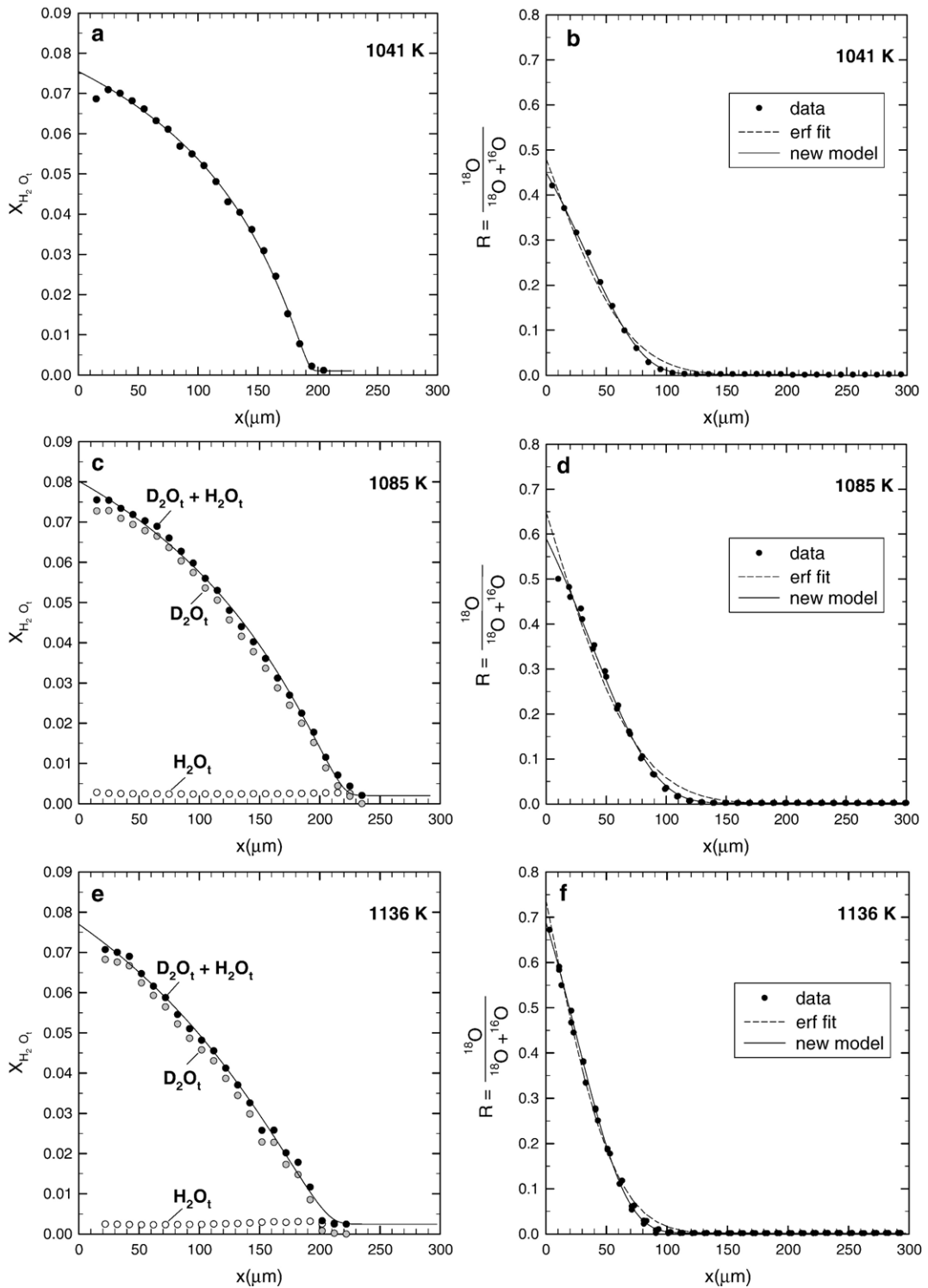


Fig. 1. a–e.  $\text{H}_2\text{O}_t$  and  $^{18}\text{O}$  profiles generated by hydrothermal experiments. The  $\text{H}_2\text{O}_t$  profiles (sum of both isotopes) clearly differ from an error function profile, and no error function fit is tried. The  $^{18}\text{O}$  profiles appear to be of error function shape, but the error function fit (dashed curves) shows small systematic deviation, especially at  $x \approx 80$  to  $100 \mu\text{m}$  (low  $\text{H}_2\text{O}_t$  content) where the data show more rapid decrease towards the background value of 0.002. The solid curves are fits of both  $\text{H}_2\text{O}_t$  and  $R$  profiles by assuming  $\text{H}_2\text{O}_m$  is the only diffusing species and  $D_{\text{H}_2\text{O}_m} = D_0 \exp(aX_{\text{H}_2\text{O}_t})$ . The best-fit values of  $a$  and  $D_0$  are listed in Table 2. No adjustments to the surface position of the  $\text{H}_2\text{O}_t$  profile were made to match  $D_{\text{H}_2\text{O}_m}$  from the  $\text{H}_2\text{O}_t$  and  $R$  profiles.

profile extends to about one half of the  $H_2O_t$  profile (Fig. 1).

#### 4. Fitting concentration profiles

The model to fit the concentration profiles of both  $H_2O_t$  and  $^{18}O$  is based on Zhang et al. [1]. Assuming molecular  $H_2O$  is the diffusing species and there is local equilibrium between OH and molecular  $H_2O$  species, the diffusion equation for  $H_2O_t$  is:

$$\frac{\partial X_{H_2O_t}}{\partial t} = \frac{\partial}{\partial x} \left( D_{H_2O_m} \frac{\partial X_{H_2O_m}}{\partial x} \right), \quad (5)$$

where  $t$  is time, and  $x$  is the space coordinate along the direction of diffusion. The diffusion equation for  $R$  presuming  $H_2O_m$  is the diffusing species requires additional approximation. Assuming (i)  $^{18}O/^{16}O$  ratio is the same for different oxygen species in the melt (e.g., there is isotopic equilibrium and the fractionation factor is very close to 1) and (ii) total oxygen concentration is roughly constant, the diffusion equation for  $^{18}O$  is:

$$\frac{\partial R}{\partial t} \approx \frac{\partial}{\partial x} \left( D_{H_2O_m} \frac{\partial (R \cdot X_{H_2O_m})}{\partial x} \right) - R \frac{\partial}{\partial x} \left( D_{H_2O_m} \frac{\partial X_{H_2O_m}}{\partial x} \right). \quad (6)$$

The apparent  $D_{^{18}O}$  based on the above equation depends on various conditions. A relatively simple approximation is  $D_{^{18}O} \approx D_{H_2O_m} \cdot X_{H_2O_m}$  (i.e., Eq. (2)). Numerical simulations show that the accuracy of this approximation depends largely on  $H_2O_t$ . For example,  $D_{^{18}O}$  exceeds  $D_{H_2O_m} \cdot X_{H_2O_m}$  by less than 10% relative when  $X_{H_2O_t} < 0.01$ , but by up to 40% when  $X_{H_2O_t}$  increases to 0.1.

In fitting experimental profiles, we applied Eqs. (5) and (6) directly without approximations. A nonlinear multivariable regression program was used to minimize the sum of residual squares [25,28]. For internal consistency and to enable comparison to our previous water diffusion study [28] we have used the equilibrium constant for water speciation in rhyolitic melts from

Zhang [40].  $D_{H_2O_m}$  in the equations is assumed to increase exponentially with  $H_2O_t$  content [28–31]:

$$D_{H_2O_m} = D_0 \exp(aX_{H_2O_t}), \quad (7)$$

where  $a$  and  $D_0$  are parameters to be obtained by fitting the profiles. Using parameter  $a$  obtained from the  $H_2O_t$  profile, the  $^{18}O$  profile is fit separately to obtain  $D_0$ . If the model is correct and the data were perfect,  $D_0$  obtained from the  $^{18}O$  profile should be the same as that from the  $H_2O_t$  profile.

Best fits of the original data are shown as solid curves in Fig. 1. The fits to both  $H_2O_t$  profile and  $R$  profile are nearly perfect. The fit to the  $R$  profile (solid curves in Fig. 1b, d and f) captures the small deviation from the error function fit (dashed curves in Fig. 1b, d, and f). Further calculations using the theory (but not related to the specific experiments reported here) show that the  $R$  profile can deviate from an error function either by terminating more quickly, or with a long tail. A long tail could result from at least two scenarios: (i) when there is local isotopic equilibrium near the surface because of high  $H_2O$  content, but little isotopic exchange at low  $H_2O$  content; or (ii) when the initial  $H_2O$  content in the sample is greater than the surface content. Hence, deviation from an error function does not necessarily reflect multiple diffusion mechanisms.

The values of  $D_{H_2O_m}$  derived from the  $H_2O_t$  profile differ from those derived from the  $^{18}O$  profile by only 3% to 24% (last columns in Table 2). Such a small difference can be accounted for by measurement uncertainty, including those on the position of the interface, spatial resolution, concentrations (such as that due to calibration), etc. For example, the “measured” interface position may differ from the real position by up to 5  $\mu m$  because of edge chipping for SIMS measurements of  $^{18}O$  profiles, and by up to 20  $\mu m$  for FTIR measurements of  $H_2O_t$  profiles because the edge may not be perfectly vertical and planar [25,28]. Furthermore, measurement spot size is finite, with the spatial resolution of 5–10  $\mu m$  for SIMS and 30  $\mu m$  for FTIR measurements. Considering these uncertainties, we

Table 3  
Calculated diffusivities (in  $\mu m^2/s$ )

Exp #	$T$ (K)	Surface $X_{H_2O_t}$	Surface $X_{H_2O_t}$ <sup>a</sup>	$D_{H_2O_m}$ at surface <sup>b</sup>	$D_{H_2O_t}$ at surface <sup>b</sup>	$D_{^{18}O}$ at surface <sup>b</sup>	$D_{^{18}O}$ based on erf fit
1	1041	0.0756	0.0295	24.7	14.4	0.73	0.63±0.07
2	1085	0.0775	0.0290	27.8	15.8	0.81	0.93±0.06
3	1136	0.0750	0.0260	45.5	24.4	1.18	1.06±0.04

Notes. The errors for the calculated diffusivities are estimated to be <30%.

<sup>a</sup> Calculated after Zhang et al. [49].

<sup>b</sup> Calculated using parameters given in Table 2.



adjusted  $H_2O_t$  and  $R$  profiles to see whether it is possible to use the same expression of  $D_{H_2O_m}$  to fit both profiles. This turned out to be relatively easy to achieve. For example, if we adjust only the interface position of the  $H_2O_t$  profile, both  $H_2O_t$  and  $R$  profiles would be fit by exactly the same expression of  $D_{H_2O_m}$  with adjustment of the interface position of the  $H_2O_t$  profile by  $2\ \mu\text{m}$  for the 1041 K experiment, by  $7\ \mu\text{m}$  for the 1136 K experiment, and by  $14\ \mu\text{m}$  for the 1085 K experiment. That is, with very minor adjustments that are within measurement uncertainty,  $^{18}\text{O}$  diffusion profile can be directly calculated with no free parameters from  $D_{H_2O_m}$  obtained from  $H_2O_t$  profile.

As shown in Table 3, the approximate  $D_{^{18}\text{O}}$  values obtained by fitting an error function to the  $R$  profiles are in good agreement with those calculated from the approximate theoretical relation  $D_{^{18}\text{O}} \approx D_{H_2O_m} \cdot X_{H_2O_m}$  using  $X_{H_2O_m}$  at the surface. Furthermore, because  $D_{^{18}\text{O}}$  is roughly proportional to  $X_{H_2O_m}$  and because  $X_{H_2O_m}$  decreases from the surface to the interior, the approximate values of  $D_{^{18}\text{O}}$  obtained by fitting an error function to the  $R$  profiles would be expected to be slightly less than those from theoretical calculation, consistent with the results shown in Table 3.

### 5. Comparison with previous data and with Eyring diffusivity

The new experimental data for  $D_{H_2O_t}$  and  $D_{H_2O_m}$  at 1 wt.%  $H_2O_t$  obtained in this study are in excellent agreement with those predicted from Zhang and Behrens [28] (Fig. 2a). On the other hand, at 4 wt.%  $H_2O_t$  the new diffusivity data are systematically higher by a factor of 2 (Fig. 2b). There are two possible explanations. One explanation is in the experimental approach. The model of Zhang and Behrens [28] is based on dehydration and diffusion couple experiments whereas in the present study the sorption technique was employed. Although the model used by Zhang and Behrens [28] and by this study does not depend on sorption or dehydration experiments, there might be experimental aspects that were overlooked. For example, in the sorption experiments, there could be surface dissolution during the experiment and re-deposition during quenching. The second, and the more likely explanation, is that the pressure effect in the model is not well constrained, as also pointed out in that paper [28]. Most data with high  $H_2O_t$  contents were for pressures of 500 MPa, with only two experiments at 250 MPa. Low pressure experiments (0.1 MPa) are limited to at most 1.7 wt%  $H_2O_t$  with only two samples having water contents exceeding 1 wt.%. The new

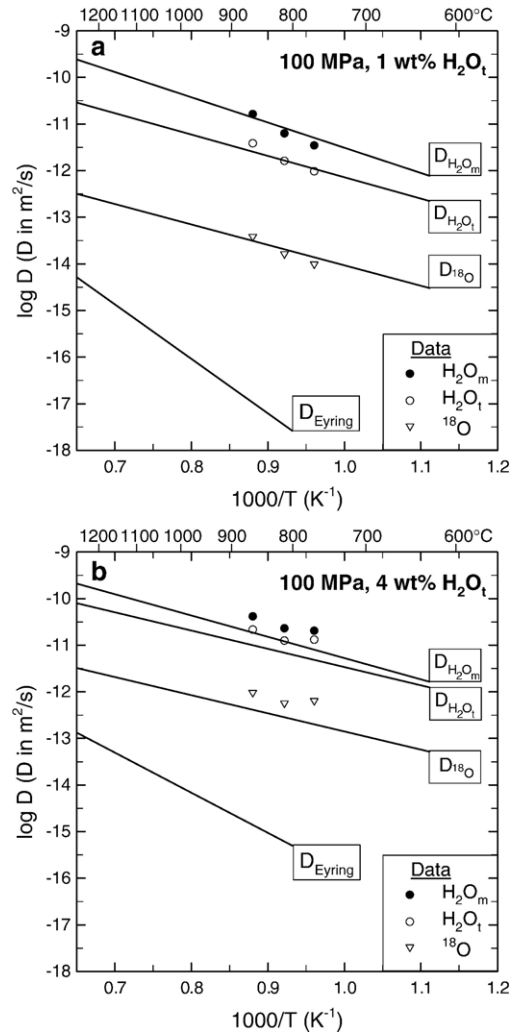


Fig. 2. a, b. Comparison of diffusivities of molecular  $H_2O$ , total  $H_2O$ ,  $^{18}\text{O}$  under hydrothermal conditions, and Eyring diffusivities at 1 and 4 wt.%  $H_2O_t$  and 100 MPa. Solid curves for  $D_{H_2O_m}$ ,  $D_{H_2O_t}$  is based on the model of Zhang and Behrens [28] and  $D_{^{18}\text{O}}$  is calculated using  $D_{^{18}\text{O}} \approx D_{H_2O_m} \cdot X_{H_2O_m}$ .

results suggest that the pressure dependence of water diffusivity at high water content is more pronounced than predicted. Further research is required to resolve this minor discrepancy. Because the comparisons of  $^{18}\text{O}$  and  $H_2O_t$  profiles are made for the same experiments, the discrepancy discussed above does not affect the conclusion that  $^{18}\text{O}$  is transported by molecular  $H_2O$  in rhyolitic melt under hydrothermal conditions.

Fig. 2 shows that  $D_{^{18}\text{O}}$  in hydrous rhyolitic melts is only 1–2 orders of magnitude less than  $D_{H_2O_t}$  but more than three orders of magnitude greater than the

diffusivity calculated from viscosity using the Eyring-relationship:

$$D = \frac{k \cdot T}{\lambda \cdot \eta} \quad (8)$$

where  $k$  is Boltzmann constant,  $\lambda$  is jumping distance, and  $\eta$  is viscosity of hydrous rhyolitic melt [43,44]. The Eyring equation has been shown to be a powerful approach to link melt viscosity to the diffusivity of network formers [45–48], the crucial parameter being the jumping distance. Agreement within a factor of 2 between viscosity and diffusivity data was found for  $\lambda$  values close to the diameter of the silicon tetrahedron [45]. In our calculations we have used  $\lambda = 2 \text{ \AA}$  which was derived by comparison of diffusion couple experiments in the system Ab-Or-Qz (Behrens, unpublished data) with viscosity data for a haplogranitic melt [44]. For anhydrous silicate melts the Eyring diffusivity was found to be close to the diffusivity of oxygen [44,45]. This is obviously not the case for hydrous melts in which oxygen diffusion is decoupled from diffusion of network cations (Al, Si). Due to the large difference between  $D_{^{18}\text{O}}$  and Eyring diffusivity, the contribution of  $\text{H}_2\text{O}$  as carrier for oxygen is expected to dominate  $D_{^{18}\text{O}}$  even at low  $\text{H}_2\text{O}$  content down to ppm level (note that Eyring diffusivity obtained from viscosity also depends on  $\text{H}_2\text{O}$  content).

## 6. Conclusions

The above results confirm that molecular  $\text{H}_2\text{O}$  is the carrier for oxygen transport in rhyolitic melt under hydrothermal conditions. We further infer that molecular  $\text{H}_2\text{O}$  diffusion controls oxygen transport in other silicate melts and glasses, and hydrous species (either molecular  $\text{H}_2\text{O}$ , or OH, or  $\text{H}_3\text{O}^+$ , or a combination of these) are responsible for oxygen transport in silicate minerals that contain hydrous component under hydrothermal conditions [1]. Previously reported oxygen “self” diffusion data under wet conditions are due to chemical diffusion of  $\text{H}_2\text{O}$  (i.e., due to the concentration gradient of  $\text{H}_2\text{O}_m$ , sometimes at minute concentration level), instead of true “self” diffusion (due to the isotopic gradient in a chemically uniform system). Nevertheless, application of the data to calculate rates for oxygen isotope exchange under hydrothermal conditions is still valid as long as they are applied under identical conditions (e.g., the same  $T$ ,  $P$ , fluid pressure and composition). Under different conditions (e.g., such as different fluid pressure), the applicable diffusivities need to be obtained by interpolation or extrapolation based on theoretical considerations that  $D_{^{18}\text{O}} \approx D_{\text{H}_2\text{O}_m} \cdot X_{\text{H}_2\text{O}_m}$ .

In the context of the above conclusions,  $^{18}\text{O}$  “self” diffusivity can be calculated from  $\text{H}_2\text{O}$  diffusion data, and vice versa. Data on  $\text{H}_2\text{O}$  diffusion in rhyolitic melt are extensive [25,27,28] and references therein] with additional data from this study. Diffusivity data in other melts are also accumulating [26,29–31], which can be used to estimate  $^{18}\text{O}$  diffusivity in these melts using Eq. (2) provided that water speciation data for the melt are available. In the future it will be an important task to investigate  $\text{H}_2\text{O}$  and  $^{18}\text{O}$  diffusion simultaneously in minerals such as feldspar or quartz to confirm the validity of this hypothesis for minerals.

## Acknowledgements

This study was supported by German DFG and the US NSF (EAR-0228752; EAR-0537598). We thank the constructive and insightful comments of an anonymous reviewer.

## References

- [1] Y. Zhang, E.M. Stolper, G.J. Wasserburg, Diffusion of a multi-species component and its role in the diffusion of water and oxygen in silicates, *Earth Planet. Sci. Lett.* 103 (1991) 228–240.
- [2] S.C. Elphick, C.M. Graham, The effect of hydrogen on oxygen diffusion in quartz: evidence for fast proton transients? *Nature* 335 (1988) 243–245.
- [3] B.J. Giletti, M.P. Semet, R.A. Yund, Studies in diffusion—III. Oxygen in feldspars: an ion microprobe determination, *Geochim. Cosmochim. Acta* 42 (1978) 45–57.
- [4] B.J. Giletti, R.A. Yund, Oxygen diffusion in quartz, *J. Geophys. Res.* 89 (1984) 4039–4046.
- [5] B.J. Giletti, K.C. Hess, Oxygen diffusion in magnetite, *Earth Planet. Sci. Lett.* 89 (1988) 115–122.
- [6] J.R. Farver, Oxygen self-diffusion in diopside with application to cooling rate determinations, *Earth Planet. Sci. Lett.* 92 (1989) 386–396.
- [7] S.M. Fortier, B.J. Giletti, Volume self-diffusion of oxygen in biotite, muscovite, and phlogopite micas, *Geochim. Cosmochim. Acta* 55 (1991) 1319–1330.
- [8] E.B. Watson, D.J. Cherniak, Oxygen diffusion in zircon, *Earth Planet. Sci. Lett.* 148 (1997) 527–544.
- [9] J.R. Farver, R.A. Yund, The effect of hydrogen, oxygen, and water fugacity on oxygen diffusion in alkali feldspar, *Geochim. Cosmochim. Acta* 54 (1990) 2953–2964.
- [10] D. Griggs, Hydrolytic weakening of quartz and other silicates, *Geophys. J. R. Astron. Soc.* 14 (1967) 19–31.
- [11] A.K. Kronenberg, S.H. Kirby, R.D. Aines, G.R. Rossman, Solubility and diffusional uptake of hydrogen in quartz at high water pressures: implications for hydrolytic weakening, *J. Geophys. Res.* 91 (1986) 12,723–12,741.
- [12] J.R. Goldsmith, The role of hydrogen in promoting Al–Si interdiffusion in albite ( $\text{NaAlSi}_3\text{O}_8$ ) at high pressures, *Earth Planet. Sci. Lett.* 80 (1986) 135–138.
- [13] R.A. Yund, Interdiffusion of NaSi–CaAl in peristerite, *Phys. Chem. Miner.* 13 (1986) 11–16.

- [14] G. Baschek, W. Johannes, The estimation of NaSi–CaAl interdiffusion rates in peristerites by homogenization experiments, *Eur. J. Mineral.* 7 (1995) 295–307.
- [15] A.H. Eward, The effect of pressure on oxygen isotope exchange in silicates, *Chem. Geol.* 49 (1985) 179–185.
- [16] B.E. Hobbs, Point defect chemistry of minerals under hydrothermal environment, *J. Geophys. Res.* 89 (1984) 4026–4038.
- [17] D.R. Cole, S. Chakraborty, Rates and mechanisms of isotopic exchange, *Rev. Mineral. Geochem.* 43 (2001) 83–223.
- [18] R. Pfeffer, M. Ohring, Network oxygen exchange during water diffusion in SiO<sub>2</sub>, *J. Appl. Phys.* 52 (1981) 777–784.
- [19] C.M. Graham, S.C. Elphick, A re-examination of the role of hydrogen in Al–Si interdiffusion in feldspars, *Contrib. Mineral. Petrol.* 104 (1990) 481–491.
- [20] C.M. Graham, S.C. Elphick, Hydrogen in feldspars and related silicates, in: I. Parsons (Ed.), *Feldspars and their Reactions*, NATO ASI Series, Kluwer, 1994.
- [21] K. Wright, R. Freer, C.R.A. Catlow, Water-related defects and oxygen diffusion in albite: a computer simulation study, *Contrib. Mineral. Petrol.* 125 (1996) 161–166.
- [22] J.D.C. McConnell, The role of water in oxygen isotope exchange in quartz, *Earth Planet. Sci. Lett.* 136 (1995) 97–107.
- [23] R.H. Doremus, The diffusion of water in fused silica, in: J.W. Mitchell, R.C. Devries, R.W. Roberts, P. Cannon (Eds.), *Reactivity of Solids*, Wiley, 1969.
- [24] R.H. Doremus, *Glass Science*, Wiley and Sons, New York, 1973 379 pp.
- [25] Y. Zhang, E.M. Stolper, G.J. Wasserburg, Diffusion of water in rhyolitic glasses, *Geochim. Cosmochim. Acta* 55 (1991) 441–456.
- [26] Y. Zhang, E.M. Stolper, Water diffusion in basaltic melts, *Nature* 351 (1991) 306–309.
- [27] M. Nowak, H. Behrens, An experimental investigation on diffusion of water in haplogranitic melts, *Contrib. Mineral. Petrol.* 126 (1997) 365–376.
- [28] Y. Zhang, H. Behrens, H<sub>2</sub>O diffusion in rhyolitic melts and glasses, *Chem. Geol.* 169 (2000) 243–262.
- [29] C. Freda, D.R. Baker, C. Romano, P. Scarlato, Water diffusion in natural potassic melts, *Geol. Soc. Spec. Publ.* 213 (2003) 53–62.
- [30] Y. Liu, Y. Zhang, H. Behrens, H<sub>2</sub>O diffusion in dacitic melt, *Chem. Geol.* 209 (2004) 327–340.
- [31] H. Behrens, Y. Zhang, Z. Xu, H<sub>2</sub>O diffusion in dacitic and andesitic melts, *Geochim. Cosmochim. Acta* 68 (2004) 5139–5150.
- [32] H. Behrens, M. Nowak, The mechanisms of water diffusion in polymerized melts, *Contrib. Mineral. Petrol.* 126 (1997) 377–385.
- [33] R.H. Doremus, Diffusion of water in rhyolite glass: diffusion-reaction model, *J. Non-Cryst. Solids* 261 (2000) 101–107.
- [34] J. Crank, *The Mathematics of Diffusion*, 2nd edition Clarendon press, Oxford, 1975 414 pp.
- [35] M. Leschik, G. Heide, G.H. Frischat, H. Behrens, M. Wiedenbeck, N. Wagner, K. Heide, H. Geißler, U. Reinholz, Determination of H<sub>2</sub>O and D<sub>2</sub>O contents in rhyolitic glasses using KFT, NRA, EGA, IR spectroscopy, and SIMS, *Phys. Chem. Glasses* 45 (2004) 238–251.
- [36] F. Holtz, H. Behrens, D.B. Dingwell, W. Johannes, H<sub>2</sub>O solubility in haplogranitic melts: compositional, pressure, and temperature dependence, *Am. Mineral.* 80 (1995) 94–108.
- [37] P. Papale, Modeling of the solubility of a one-component H<sub>2</sub>O or CO<sub>2</sub> fluid in silicate liquids, *Contrib. Mineral. Petrol.* 126 (1997) 237–251.
- [38] G. Moore, T. Vennemann, I.S.E. Carmichael, An empirical model for the solubility of H<sub>2</sub>O in magmas to 3 kilobars, *Am. Mineral.* 83 (1998) 36–42.
- [39] S. Yamashita, Experimental study of the effect of temperature on water solubility in natural rhyolite melt to 100 MPa, *J. Petrol.* 40 (1999) 1497–1507.
- [40] Y. Zhang, H<sub>2</sub>O in rhyolitic glasses and melts: measurement, speciation, solubility, and diffusion, *Rev. Geophys.* 37 (1999) 493–516.
- [41] N. Tamic, H. Behrens, F. Holtz, The solubility of H<sub>2</sub>O and CO<sub>2</sub> in rhyolitic melts in equilibrium with a mixed CO<sub>2</sub>–H<sub>2</sub>O fluid phase, *Chem. Geol.* 174 (2001) 333–347.
- [42] Y. Liu, Y. Zhang, H. Behrens, Solubility of H<sub>2</sub>O in rhyolitic melts at low pressures, *J. Volcanol. Geotherm. Res.* 143 (2005) 219–235.
- [43] F. Schulze, H. Behrens, F. Holtz, J. Roux, W. Johannes, The influence of water on the viscosity of a haplogranitic melt, *Am. Mineral.* 81 (1996) 1155–1165.
- [44] Y. Zhang, Z. Xu, Y. Liu, Viscosity of hydrous rhyolitic melts inferred from kinetic experiments, and a new viscosity model, *Am. Mineral.* 88 (2003) 1741–1752.
- [45] S. Chakraborty, Diffusion in silicate melts, *Rev. Miner.* 32 (1995) 411–503.
- [46] J. Koepke, H. Behrens, Trace element diffusion in andesitic melts — an application of synchrotron X-ray fluorescence analysis, *Geochim. Cosmochim. Acta* 65 (2001) 1481–1498.
- [47] B.T. Poe, P.F. McMillan, D.C. Rubie, S. Chakraborty, J. Yarger, J. Diefenbacher, Silicon and oxygen self-diffusivities in silicate liquids measured to 15 gigapascals and 2800 Kelvin, *Science* 276 (1997) 1245–1248.
- [48] J.E. Reid, B.T. Poe, D.C. Rubie, N. Zotov, M. Wiedenbeck, The self-diffusion of silicon and oxygen in diopside (CaMgSi<sub>2</sub>O<sub>6</sub>) liquid up to 15 GPa, *Chem. Geol.* 174 (2001) 77–86.
- [49] Y. Zhang, R. Belcher, P.D. Ihinger, L. Wang, Z. Xu, S. Newman, New calibration of infrared measurement of dissolved water in rhyolitic glasses, *Geochim. Cosmochim. Acta* 61 (1997) 3089–3100.